Mononuclear and Binuclear Chromium(III) Picolinate Complexes

Diane M. Stearns[1a] and William H. Armstrong*[,1b]

Department of Chemistry, University of California, Berkeley, California 94720

Received June 5, 1991

The chromium(III) picolinate complexes $[Cr(pic)_3]$ (**1**) and $[Cr(pic)_2OH]_2$ (**2**) (where pic = 2-carboxypyridine) have been isolated from the reaction of chromium(III) chloride and picolinic acid in aqueous solution. The monomeric complex $\mathbf{1}\cdot H_2O$ ($CrC_{18}H_{14}N_3O_7$) crystallizes in the monoclinic space group $C2/c$ with $a = 30.219$ (3) Å, $b = 8.529$ (1) Å, $c = 13.942$ (2) Å, $\beta = 95.141$ (1)°, $V = 3579$ (2) Å^3, $Z = 4$, $R = 0.032$, and $R_w = 0.043$ for 1815 reflections ($I > 3\sigma(I)$). The binuclear complex $\mathbf{2}\cdot 5H_2O$ ($Cr_2C_{24}H_{28}N_4O_{15}$) crystallizes in the monoclinic space group $P2_1/n$ with $a = 12.569$ (2) Å, $b = 18.839$ (3) Å, $c = 13.000$ (4) Å, $\beta = 105.823$ (3)°, $V = 2962$ (2) Å^3, $Z = 8$, $R = 0.046$, $R_w = 0.067$ for 3250 reflections ($I > 3\sigma(I)$). The mononuclear complex **1** is the meridional isomer, not the facial isomer as previously assumed. For **2** the bridging geometry is as follows: Cr–Cr = 2.999 (1) Å; Cr–O(bridge) range = 1.934 (3)–1.980 (3) Å; Cr–O–Cr = 99.0 (1), 101.6(1)°; O–Cr–O = 79.4 (1), 79.9 (1)°. Magnetic susceptibility data for **2** were measured from 280 to 6 K and can be fit using an isotropic spin-exchange Hamiltonian, $\mathcal{H} = -2J\hat{S}_1\cdot\hat{S}_2$, with a weak antiferromagnetic interaction ($J = -8.02$ (4) cm^{-1}), $g = 1.844$, and a 2.23 (4) mol % paramagnetic impurity. The extent of magnetic coupling in **2** is compared to predictions made by the Glerup–Hodgson–Pedersen (GHP) equation. Compounds **1** and **2** are discussed in the general context of biologically active chromium.

Introduction

Among the motivating factors for studying chromium(III) picolinate coordination chemistry, two that we are concerned with are (i) the clarification of misconceptions in the literature regarding the prevalent isomer for $[Cr(pic)_3]$ and (ii) the evaluation of these complexes as potential bioavailable sources of chromium, an essential trace element.[2a–c] While claims have been made regarding the biological efficacy of chromium tris(picolinate),[3a,b] the issue is by no means settled (vide infra).

Prior to the work described herein, the only structurally characterized chromium picolinate complex was the hexakis(picolinato) μ_3-oxo trinuclear species $[Cr_3O(Hpic)_6(H_2O)_3](ClO_4)_7\cdot 6NaClO_4\cdot 3H_2O$[4,5] which bears resemblance to other compounds that contain the $\{Cr_3O\}^{n+}$ core.[6a,b] We report here the spectroscopic, structural and magnetic properties of $[Cr(pic)_3]$ (**1**), and $[Cr(pic)_2(OH)]_2$ (**2**). Since the Cr(III) ion (d^3) is relatively substitutionally inert, an understanding of the structures of these complexes may ultimately be useful in rationalizing the uptake and function (or lack thereof) of chromium–picolinate complexes as biologically active sources of chromium.

As implied above, chromium complexes of picolinic acid have been previously described in the literature.[7–10] In cases where the geometrical isomerism was mentioned, the red $[Cr(pic)_3]$ complex was assigned as the facial isomer[7,9] based on comparison of its color to similar complexes such as $[Co(gly)_3]$,[11] $[Co(pic)_3]$,[12] and $[Cr(gly)_3]$.[13] Yuen et al.[9] included the red $[Cr(pic)_3]$ in a spectrochemical series of CrN_3O_3 complexes with tris(amino carboxylate) ligands, assuming $[Cr(pic)_3]$ to be the facial isomer. Oki and Yoneda[14] isolated a purple complex from the reaction of $[Cr(NH_3)_6](NO_3)_3$ with L-proline, which they demonstrated to be the bis(μ-hydroxo)tetrakis(L-prolinato)dichromium(III) dimer using X-ray crystallography. Prior to the structure solution they assumed the purple complex to be either the meridional monomer or the bis(μ-hydroxo) dimer since "all facial isomers of tris(aminoacidato)chromium(III) complexes are reported to be either pink or red in color."[14]

The crystal structure of the red $[Cr(pic)_3]$ complex has been solved, and we find it to be the meridional isomer. There are at least two common assumptions in the literature that have been disproven by the characterization of the complexes described here. The first is that meridional isomers of CrL_3 (where L = a bidentate amino carboxylate ligand) are purple and that only facial isomers are red;[7,14] the second, that the facial isomers are generally more stable than the meridional ones.[7,15,16]

The magnetic exchange interaction in **2** is discussed in relation to the Glerup–Hodgson–Pedersen (GHP) model[17] which corre-

(1) (a) Present address: Department of Chemistry, Dartmouth College, Hanover, NH 03755. (b) Present address: Department of Chemistry, Merkert Chemistry Center, Boston College, Chestnut Hill, MA 02167.
(2) (a) Schwarz, K.; Mertz, W. *Arch. Biochem. Biophys.* **1957**, *72*, 515–518. (b) Schwarz, K.; Mertz, W. *Arch. Biochem. Biophys.* **1959**, *85*, 292–295. (c) Mertz, W. *Science* **1981**, *213*, 1332–1338.
(3) (a) Evans, G. US Patent 4,315,927, 1982. (b) Press, R. I.; Geller, J.; Evans, G. W. *West. J. Med.* **1990**, *152*, 41–55.
(4) Bradshaw, J. E.; Grossie, D. A.; Mullica, D. F.; Pennington, D. E. *Inorg. Chim. Acta* **1988**, *141*, 41–47.
(5) Abbreviations used in this paper: GTF, glucose tolerance factor; gly, glycinate; pic, picolinate, anion of 2-carboxypyridine; NMR, nuclear magnetic resonance; DMF, *N*,*N*-dimethylformamide; DMSO, dimethyl sulfoxide; THF, tetrahydrofuran.
(6) (a) Chang, S. C.; Jeffrey, G. A. *Acta Crystallogr., Sect. C* **1970**, *480*, 673–683. (b) Gonzalez-Veraga, E.; Hegenauer, J.; Saltman, P.; Sabat, M.; Ibers, J. A. *Inorg. Chim. Acta* **1982**, *66*, 115–118.
(7) Israily, N. *C. R. Acad. Sci. Paris* **1966**, *262*, 1426–1428.
(8) Chatterjee, B. *J. Indian Chem. Soc.* **1976**, *53*, 1212–1213.
(9) Yuen, G.; Heaster, H.; Hoggard, P. E. *Inorg. Chim. Acta* **1983**, *73*, 231–234 and references therein.
(10) Dorsett, T. E.; Walton, R. A. *J. Chem. Soc., Dalton Trans.* **1976**, 347–350.
(11) Gerlach, H.; Mullen, K. *Helv. Chim. Acta* **1974**, *57*, 2234–2237. The red facial isomer and purple meridional isomer were distinguished by ^{13}C NMR.
(12) Pelizzi, C.; Pelizzi, G. *Transition Met. Chem.* (*Weinheim, Ger.*) **1981**, *6*, 315–316. The purple complex was structurally characterized as the meridional isomer.
(13) Bryan, R. F.; Greene, P. T.; Stokely, P. F.; Wilson, E. W. *Inorg. Chem.* **1971**, *10*, 1468–1473. The red complex was structurally characterized as the facial isomer.
(14) Oki, H.; Yoneda, H. *Inorg. Chem.* **1981**, *20*, 3875–3879.
(15) Gillard, R. D.; Laurie, S. H.; Price, D. C.; Phipps, D. A.; Weick, C. F. *J. Chem. Soc., Dalton Trans.* **1974**, 1385–1396.
(16) Wallace, W. M.; Hoggard, P. E. *Inorg. Chim. Acta* **1982**, *65*, L3–L5.
(17) Glerup, J.; Hodgson, D. J.; Pedersen, E. *Acta Chem. Scand.* **1983**, *A37*, 161–164. For $\mathcal{H} = J\hat{S}_1\cdot\hat{S}_2$

$$J = e^{-a(r-1.8)}\left[\frac{b\cos^4\theta}{\{(1-\sin^2\theta)/\tan^2(\phi/2)\}^2} - \frac{c\sin^2\phi}{(1-\cos\phi)^2}\right]$$

where r = Cr–O bond length (Å), ϕ = Cr–O–Cr angle (deg), θ = angle of O–H bond out of the Cr_2O_2 plane (deg), $a = 19$ Å^{-1}, $b = 611$ cm^{-1}, and $c = 172$ cm^{-1}.

0020-1669/92/1331-5178$03.00/0

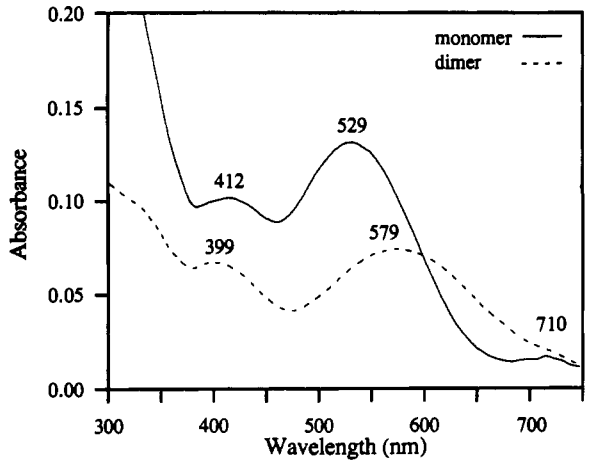

Figure 1. Diffuse reflectance spectra of $[Cr(pic)_3]$ (**1**) (–), and $[Cr(pic)_2OH]_2$ (**2**) (– – –) with absorbance maxima labeled.

lates structural and magnetic properties for dihydroxo-bridged Cr(III) dimers. The results presented here are briefly discussed in light of the literature on the biological role of chromium.

Experimental Section

General Procedures. Materials were purchased from commercial sources and used without further purification. Elemental analyses were performed by the UC Berkeley Microanalytical Laboratory. Infrared spectra (IR) were recorded on a Nicolet 5DX Fourier transform infrared spectrometer. Optical spectra were recorded on a Perkin-Elmer Lambda 9 spectrophotometer. Solid-state magnetic susceptibility measurements of **1** (25 °C) and **2** (variable temperature) were carried out on a 800 VTS-50 SQUID magnetometer (SHE Corp.) using a field strength of 5kG. A diamagnetic correction of -204×10^{-6} cm^3 mol^{-1} was calculated from Pascal's constants[18] and applied to the magnetic susceptibility measurement of **1**. Since the crystal structure of **2** showed several disordered water molecules, a microcrystalline portion was ground to a powder and heated under vacuum for 24 h to remove the water of hydration[15] prior to the magnetic susceptibility measurements. Elemental analysis of the sample used for magnetic measurements confirmed the loss of all water, and calculations were carried out using the molecular weight of the anhydrous dimer (626.42 g/mol). A total of 35 data points were taken for a 34.08-mg sample over the temperature range 6 K $\leq T \leq$ 280 K. A correction was made over the temperature range for the moment of the Kel-F sample holder. For **2**, a diamagnetic correction of -288×10^{-6} cm^3 mol^{-1} was calculated from Pascal's constants.[18] Data were fit to the expression for χ_m vs T for an $S_1 = S_2 = {}^3/_2$ dimer derived from the isotropic spin-exchange Hamiltonian $\mathcal{H} = -2J\hat{S}_1\cdot\hat{S}_2$[17] (see below) and refined using a nonlinear least-squares technique.

Preparation of Compounds. $[Cr(pic)_3]\cdot H_2O$ (1). An 8-mL aliquot of a solution that was 0.16 M in $Cr(NO_3)_3\cdot 9H_2O$ and 0.55 M in picolinic acid in 0.16 M aqueous HNO_3 (pH 1) was stirred for 30 min at 60 °C. The red-purple solution was filtered and allowed to stand at room temperature for 2 weeks, during which time a red microcrystalline solid was obtained with some red diamond-shaped X-ray quality crystals (combined yield 48%). The dimer was not observed to form under these conditions based on examination of crystal habit and color of the product. Anal. Calcd for $CrC_{18}H_{14}N_3O_7$: Cr, 11.9; C, 49.55; H, 3.23; N, 9.63. Found: Cr, 11.3; C, 49.29; H, 3.23; N, 9.51. IR (KBr pellet, cm^{-1}): 1677 (s), 1607 (s), 1473 (m), 1327 (s), 1287 (s), 1159 (m), 1051 (m), 864 (m), 767 (m), 716 (m), 692 (m), 659 (w), 475 (s). The crystals are moderately soluble in 2 M aqueous HCl, DMF, and acetonitrile; slightly soluble in methanol; and insoluble in acetone, ethanol, DMSO, and THF. Optical spectra: diffuse reflectance against $BaSO_4$ at 379, 412, 524, 710 nm (Figure 1). UV/vis (2 M HNO_3): 406, 548 nm. The solution of **1** in 2 M HNO_3 is not stable with time due to hydrolysis (see below). Room temperature magnetic moment: 3.88 (3) μ_B.

$[Cr(pic)_2(OH)]_2\cdot 5H_2O$ (2). An aqueous solution (100 mL total volume) of 0.013 M $CrCl_3\cdot 6H_2O$, 0.035 M picolinic acid, and 0.04 M NaOH was stirred at 60 °C. The solution color changed from clear green to cloudy purple to wine red in approximately 10 min (final pH 4.1). The solution was filtered and allowed to stand at room temperature for 1 month. Large purple needles, suitable for an X-ray diffraction study were deposited over time (16% yield based on moles of Cr). Red crystals of **1** were also deposited (33% based on moles of Cr). Crystals were obtained more quickly when the ratio of ligand to chromium was greater than 2. Anal. Calcd for $Cr_2C_{24}H_{26}N_4O_{13}$: Cr, 14.5; C, 40.23; H, 3.94; N, 7.82. Found: Cr, 14.3; C, 40.20; H, 3.40; N, 7.86. IR (KBr pellet, cm^{-1}): 1665 (s), 1607 (s), 1474 (w), 1348 (s), 1293 (m), 1167 (w), 1053 (m), 864 (m), 764 (m), 716 (m), 694 (m), 658 (w), 549 (m), 463 (m). The crystals are slightly soluble in methanol, decompose in acetonitrile and DMF to give an uncolored precipitate, and are insoluble in acetone, ethanol, DMSO, and THF. Optical spectra: diffuse reflectance (against $BaSO_4$) at 265, 399, 579 nm (Figure 1). UV/vis (2 M HNO_3): 404, 566 nm.

Table I. Crystallographic Data for $[Cr(pic)_3]\cdot H_2O$ (**1**) and $[Cr(pic)_2OH]_2\cdot 5H_2O$ (**2**)[a]

	1	**2**
formula	$CrC_{18}H_{14}N_3O_7$	$Cr_2C_{24}H_{28}N_4O_{15}$
fw	436.32	716.50
temp, °C	25	−110
space group	$C2/c$	$P2_1/n$
a, Å	30.219 (3)	12.569 (2)
b, Å	8.529 (1)	18.839 (3)
c, Å	13.942 (2)	13.000 (4)
β, deg	95.141 (1)	105.823 (3)
V, Å^3	3579 (2)	2962 (2)
Z	8	4
d_{calc}, g cm^{-3}	1.619	1.605
μ, cm^{-1}	6.70	7.91
λ, Å	0.710 73	0.710 73
R	0.032	0.046
R_w	0.043	0.067

[a] Formulas used in structure solution: $R = (\sum||F_o| - |F_c||)/\sum|F_o|$; $R_w = \{[\sum w(|F_o| - |F_c|)^2]/\sum wF_o^2\}^{1/2}$. Function minimized: $\sum w(|F_o| - |F_c|)^2$; $w = 1/\sigma^2(F_o)$.

X-ray Data Collection and Structure Solutions. $[Cr(pic)_3]\cdot H_2O$. Crystals suitable for X-ray diffraction studies were grown directly from the aqueous reaction mixture. The crystal used for data collection, with final dimensions 0.3 × 0.2 × 0.1 mm, was cut from a large red diamond-shaped plate. The orientation matrix and unit cell parameters were determined from 25 machine-centered reflections with 8.0° ≤ 2θ ≤ 26.8°. The cell parameters and systematic absences showed the crystal to belong to a monoclinic system, the space group being either $C2/c$ or Cc. The centrosymmetric space group was chosen, and this choice was confirmed by the successful determination of the chromium atom position from the Patterson map and finally a structure solution with acceptable thermal parameters and geometry for octahedral Cr(III). The structure was refined by standard full-matrix least-squares and Fourier techniques with a Digital Equipment Micro-vax computer using locally modified Enraf-Nonius SDP software.[20] An empirical absorption correction was applied to the data. The positions of all remaining non-hydrogen atoms, including one water oxygen atom were determined from subsequent difference Fourier maps to give an intermediate R_F of 0.051. All hydrogen atoms were observed in the difference map, and were included at calculated positions in the structure factor calculation but not refined (C–H distance fixed at 0.95 Å, $B_{iso}(H) = 1.0B_{iso}(C)$). Using anisotropic thermal parameters for all non-hydrogen atoms, the refinement converged to give an R_F of 0.032 ($R_{wF} = 0.043$). The largest ratio of parameter shift to estimated standard deviation in the final refinement cycle was ≤0.01. A summary of crystallographic data is presented in Table I. Final positional parameters are listed in Table IIa.

$[Cr(pic)_2(OH)]_2\cdot 5H_2O$. Crystals suitable for X-ray diffraction studies were grown from the aqueous reaction mixture. The crystal used for data collection, with final dimensions 0.55 × 0.35 × 0.25 mm, was cut from a large purple needle. The orientation matrix and unit cell parameters were determined from 25 machine-centered reflections with 11.0° < 2θ < 24.8°. The diffractometer data showed the crystal to belong to the monoclinic space group $P2_1/n$. An empirical absorption correction was applied to the data. A summary of crystallographic data is presented in Table I.

(18) Selwood, P. W. *Magnetochemistry*; 2nd ed.; Interscience Publishers: New York, 1956.
(19) O'Connor, C. J. *Prog. Inorg. Chem.* **1982**, *29*, 204–283.
(20) Frenz, B. A. Structure Determination Package. B. A. Frenz and Associates, College Station, TX, and Enraf-Nonius, Delft, The Netherlands, 1985; as revised locally by Dr. Fredrick J. Hollander.

Table II. Positional Parameters and Their Estimated Standard Deviations for $[Cr(pic)_3]\cdot H_2O$ (**1**) and $[Cr(pic)_2OH]_2\cdot 5H_2O$ (**2**)

atom	*x*	*y*	*z*	B,[a] Å^2	atom	*x*	*y*	*z*	B,[a] Å^2
				(a) Compound **1**					
Cr	0.11313 (2)	0.21644 (7)	0.12783 (4)	2.27 (1)	C5	0.0459 (1)	0.4851 (4)	0.1215 (2)	2.83 (8)
O1	0.07299 (7)	0.0363 (3)	0.1131 (2)	2.74 (5)	C6	0.0309 (1)	0.0604 (4)	0.1180 (2)	2.78 (8)
O2	0.15267 (7)	0.3972 (3)	0.1315 (2)	2.82 (5)	C7	0.1473 (1)	0.3562 (4)	−0.0360 (2)	2.51 (7)
O3	0.11558 (7)	0.2172 (3)	0.2681 (2)	2.84 (5)	C8	0.1555 (1)	0.3964 (5)	−0.1281 (3)	3.41 (8)
O4	0.00299 (8)	−0.0418 (3)	0.1191 (2)	4.46 (6)	C9	0.1332 (1)	0.3160 (5)	−0.2048 (3)	3.64 (9)
O5	0.19927 (8)	0.5290 (3)	0.0456 (2)	4.57 (6)	C10	0.1031 (1)	0.2021 (4)	−0.1858 (2)	3.39 (8)
O6	0.16011 (9)	0.1671 (4)	0.4011 (2)	4.67 (7)	C11	0.0963 (1)	0.1669 (4)	−0.0908 (3)	2.96 (8)
O7W	0.1085 (1)	−0.2559 (3)	0.0511 (2)	5.02 (7)	C12	0.1692 (1)	0.4375 (4)	0.0521 (2)	2.96 (8)
N1	0.05332 (9)	0.3306 (3)	0.1198 (2)	2.35 (6)	C13	0.1809 (1)	0.0734 (4)	0.2523 (2)	2.43 (7)
N2	0.11832 (9)	0.2426 (3)	−0.0171 (2)	2.20 (6)	C14	0.2190 (1)	−0.0021 (5)	0.2894 (3)	3.57 (9)
N3	0.16790 (9)	0.0751 (3)	0.1568 (2)	2.36 (6)	C15	0.2439 (1)	−0.0820 (5)	0.2263 (3)	4.4 (1)
C1	0.0185 (1)	0.2319 (4)	0.1212 (2)	2.46 (7)	C16	0.2303 (1)	−0.0846 (5)	0.1297 (3)	4.18 (9)
C2	−0.0239 (1)	0.2839 (5)	0.1250 (3)	3.15 (8)	C17	0.1925 (1)	−0.0033 (5)	0.0978 (2)	3.30 (8)
C3	−0.0315 (1)	0.4437 (5)	0.1267 (3)	3.73 (9)	C18	0.1504 (1)	0.1591 (4)	0.3135 (2)	2.87 (8)
C4	0.0038 (1)	0.5464 (4)	0.1248 (3)	3.29 (8)					
				(b) Compound **2**					
Cr1	−0.01310 (5)	0.16559 (3)	0.46253 (5)	2.67 (1)	N4	0.3019 (3)	0.1107 (2)	0.3492 (3)	3.59 (8)
Cr2	0.18043 (5)	0.17856 (4)	0.37047 (5)	3.00 (1)	C1	−0.1951 (3)	0.0906 (2)	0.3234 (3)	2.90 (9)
O1	0.0975 (2)	0.1047 (1)	0.4221 (2)	2.91 (6)	C2	−0.2793 (4)	0.0704 (2)	0.2383 (3)	3.9 (1)
O2	0.0723 (2)	0.2366 (1)	0.4123 (2)	3.26 (6)	C3	−0.3022 (4)	0.1112 (3)	0.1465 (4)	4.5 (1)
O3	−0.0885 (2)	0.0825 (2)	0.5033 (2)	3.14 (6)	C4	−0.2386 (4)	0.1689 (3)	0.1428 (3)	4.0 (1)
O4	−0.2168 (2)	−0.0006 (2)	0.4427 (2)	4.12 (7)	C5	−0.1541 (3)	0.1864 (2)	0.2302 (3)	3.16 (9)
O5	−0.1110 (2)	0.2367 (2)	0.4981 (2)	3.58 (7)	C6	−0.1663 (3)	0.0529 (2)	0.4294 (3)	3.21 (9)
O6	−0.1255 (3)	0.3171 (2)	0.6181 (3)	6.22 (9)	C7	0.0193 (3)	0.2324 (2)	0.6653 (3)	3.7 (1)
O7	0.0941 (2)	0.1670 (2)	0.2214 (2)	4.36 (8)	C8	0.0590 (4)	0.2513 (3)	0.7728 (4)	5.7 (1)
O8	0.0646 (3)	0.2091 (3)	0.0565 (3)	7.6 (1)	C9	0.1506 (4)	0.2189 (4)	0.8344 (4)	6.3 (2)
O9	0.2897 (2)	0.1888 (2)	0.5100 (2)	3.77 (7)	C10	0.2015 (4)	0.1678 (3)	0.7881 (4)	5.7 (1)
O10	0.4465 (3)	0.1450 (2)	0.6156 (3)	6.6 (1)	C11	0.1598 (4)	0.1502 (3)	0.6823 (3)	4.0 (1)
OW11	0.5108 (4)	0.1335 (2)	0.8353 (3)	8.2 (1)	C12	−0.0808 (3)	0.2660 (3)	0.5887 (3)	4.0 (1)
OW12	−0.0032 (5)	0.0069 (3)	−0.2840 (5)	8.0 (2)	C13	0.1897 (3)	0.2702 (3)	0.1980 (3)	4.2 (1)
OW13	−0.004 (1)	−0.022 (1)	−0.209 (1)	8.0 (1)*	C14	0.2115 (4)	0.3266 (3)	0.1391 (4)	5.9 (1)
OW14	0.4755 (7)	0.0293 (5)	−0.0743 (7)	8.0*	C15	0.2844 (4)	0.3774 (3)	0.1898 (4)	6.7 (1)
OW15	0.101 (1)	0.023 (1)	−0.077 (1)	8.0*	C16	0.3345 (4)	0.3709 (3)	0.2949 (4)	6.4 (1)
OW16	−0.015 (1)	0.0858 (8)	0.010 (1)	8.0*	C17	0.3120 (4)	0.3124 (3)	0.3507 (4)	5.2 (1)
OW17	−0.1319 (7)	0.4312 (5)	0.4765 (7)	8.0*	C18	0.1103 (4)	0.2119 (3)	0.1527 (4)	5.1 (1)
OW18	−0.1909 (7)	0.4394 (5)	0.5100 (7)	8.0*	C19	0.3899 (3)	0.1092 (2)	0.4337 (4)	4.1 (1)
OW19	0.096 (1)	0.060 (1)	0.002 (1)	8.0*	C20	0.4851 (4)	0.0720 (3)	0.4362 (4)	5.6 (1)
OW20	−0.157 (1)	−0.0187 (8)	0.065 (1)	8.0*	C21	0.4852 (5)	0.0319 (3)	0.3490 (5)	7.9 (2)
OW21	0.013 (2)	0.055 (1)	1.066 (2)	8.0*	C22	0.3923 (5)	0.0303 (3)	0.2611 (4)	6.6 (1)
N1	−0.1317 (2)	0.1480 (2)	0.3199 (2)	2.72 (7)	C23	0.3018 (4)	0.0718 (3)	0.2646 (4)	5.1 (1)
N2	0.0692 (3)	0.1824 (2)	0.6215 (3)	3.28 (8)	C24	0.3764 (4)	0.1510 (3)	0.5290 (4)	4.5 (1)
N3	0.2392 (3)	0.2629 (2)	0.3030 (3)	3.65 (8)					

[a] Starred values indicate atoms refined with isotropic thermal parameters. The thermal parameter given for anisotropically refined atoms is the isotropic equivalent thermal parameter defined as: $(4/3)[a^2B(1,1) + b^2B(2,2) + c^2B(3,3) + ab(\cos\gamma)B(1,2) + ac(\cos\beta)B(1,3) + bc(\cos\alpha)B(2,3)]$ where a, b, and c are real cell parameters and $B(i,j)$s are anisotropic βs.

The two unique chromium positions were determined from the Patterson map. The positions of all remaining atoms of the dimer were determined from subsequent difference Fourier maps. Refinement using anisotropic parameters for all non-hydrogen atoms in the chromium complex yielded an intermediate R_F of 0.163 (R_{wF} = 0.247). Subsequent difference Fourier maps revealed positions for water oxygen atoms in the lattice, each around an inversion center. From their interatomic distances and thermal behavior only one oxygen atom position was assigned as having full occupancy. The positions were taken from the difference map, the isotropic thermal parameters were linked to the oxygen atom at full occupancy, and the multiplicities were refined. Oxygen atoms were added, and the procedure was repeated until the highest difference peak gave an unsatisfactory thermal parameter for an oxygen atom refined at ≥0.1% occupancy. The final model contained 11 pairs of oxygen atoms with varying multiplicities, each pair related by inversion symmetry. The total sum of occupancies came to 8.3. This approach is obviously an approximation because it assumes that the water molecules all have the same thermal motion, and it models the network of water molecules in the average unit cell. While this model gives reasonable thermal parameters and the best R factor, it is inconsistent with the elemental analysis, cell volume, and measured crystal density, all of which suggest a pentahydrate. Because of some uncertainty with regard to the exact quantity of water contained in the single crystals, the magnetic measurements were carried out on an anhydrous sample (see above).

All of the protons for the chromium dimer, including those for the hydroxide bridge, were revealed by a difference Fourier map. The 12 picolinate protons were fixed at a C–H distance of 0.95 Å, with B_{iso}(H) = 1.15B_{iso}(C). The hydrogen atom positions were included in structure factor calculations but were not refined. An attempt was made to refine the protons of the hydroxide bridges; however, the positions and thermal parameters of the oxygen and hydrogen atoms began to diverge, so the hydroxide protons were included in structure factor calculations but were not refined (B_{iso}(H) = 1.15B_{iso}(O)).

After several cycles of refinement the range of ratios of parameter shift to estimated standard deviation was 0.00–0.02. The secondary extinction coefficient was refined to 9.24×10^{-8} M^{-1} cm^{-1} (6% correction). The final R_F was 0.046 (R_{wF} = 0.067). Final positional parameters are listed in Table IIb.

Results and Discussion

Synthesis of Compounds. The reaction of either chromium(III) chloride or nitrate with 2 or 3 equiv of picolinic acid and 0–3 equiv of aqueous NaOH results in varying amounts of the monomer and dimer; both are observed under all of these conditions. Crystals are obtained from a filtered solution upon standing at room temperature. The $[Cr(pic)_3]$ complex comes out of solution more readily while the dimer crystallizes a few days later. These two crystal types can be separated under a microscope for characterization. The preparations described above were found to give the highest relative yield of each desired product.

Complexes **1** and **2** were obtained from the reaction of Cr^{3+} and picolinic acid in aqueous solution. In highly acidic solution

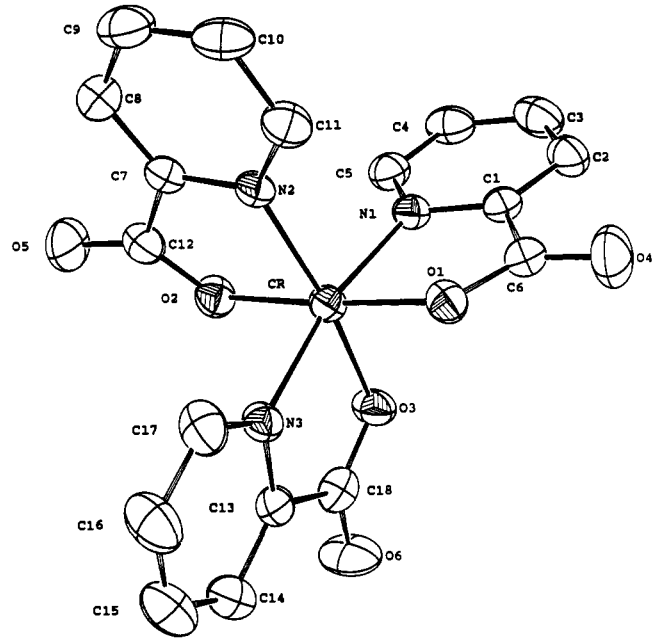

Figure 2. Structural diagram of $[Cr(pic)_3]$ (**1**). Thermal ellipsoids are at 50% probability. Hydrogen atoms and water of solvation are omitted for clarity.

(pH 1) only **1** was observed to crystallize. At pH > 4 both **1** and **2** were observed. The possibility of the existence of other more soluble species, for example a facial monomer or stereoisomers of the dimer, is not ruled out; however, only two crystal habits have been observed in our studies. Characterization of these complexes was carried out on single crystals mechanically separated under a microscope; therefore, further purification was deemed unnecessary.

The diffuse reflectance spectrum for **1** is shown in Figure 1. The visible spectrum of **1** redissolved in 2 M HNO_3(aq) gives absorbances at 406 and 548 nm. This matches the spectra reported by Nakahara[21] and Chatterjee[8] but is at odds with the λ_{max} of 515 nm reported by Yuen et al.[9] The latter authors suggest that the former solutions[8,21] are contaminated with dimer since they observe no solvent dependence for the spectrum. We observe a shift in the $^4A_2 \rightarrow {}^4T_2$ transition[22] from 548 to 566 nm over a period of 2 weeks for a solution of **1** in 2 M HCl at 25 °C, suggesting that the monomer does indeed undergo hydrolysis to the dimer even in highly acidic solution. This should be considered in any discussion of the biological activity of these molecules (see below).

Description of Structures. $[Cr(pic)_3]\cdot H_2O$. The structure and labeling scheme for **1** are shown in Figure 2. The crystal structure of **1** shows the chromium to be in a roughly octahedral geometry, surrounded by three picolinate ligands such that the oxygen atoms are in a meridional configuration. Selected interatomic distances and angles are summarized in Table IIIa. Chromium(III) tris picolinate is isostructural with its cobalt(III)[12] and manganese(III)[23] analogues. Table IV provides a comparison of the metal–ligand bond lengths for the d^3, d^4, and d^6 metal complexes. The bond lengths to chromium are greater than those to cobalt, as expected from the sizes of the corresponding ionic radii.[24] The Mn(III) complex[23] shows larger bond lengths due to the tetragonal Jahn–Teller distortion expected for d^4 species. The Cr–N bond lengths for **1** range from 2.047 (2) to 2.058 (2) Å; the Cr–O bond lengths range from 1.949 (2) to 1.957 (2) Å. These are comparable to the bond lengths reported for the meridionally coordinated tris(8-quinolinato)chromium(III),[25] which has Cr–N bond lengths from 2.053 (8) to 2.075 (9) Å and Cr-O bond lengths from 1.935 (7) to 1.968 (7) Å. In **1**, the water oxygen atom is 2.88 Å from the chromium-bonded oxygen atom of ring 1 (O1), and 2.82 Å from the carboxylate oxygen atom of ring 3 (O6). The angles between the planes formed by the pyridine rings are 86.6, 83.6, and 80.8°. The dihedral angles between each pyridine ring and its coordinating oxygen are 1, 3, and 8°.

$[Cr(pic)_2(OH)_2]\cdot 5H_2O$. The structure and labeling scheme for **2** is shown in Figure 3. The geometry constists of two roughly octahedrally coordinated chromium atoms, each with two picolinate ligands and a bridging hydroxo group. Selected bond distances and angles are listed in Table IIIb. The Cr–Cr distance

Table III. Selected Intramolecular Distances (Å) and Angles (deg) for $[Cr(pic)_3]\cdot H_2O$ (**1**) and $[Cr(pic)_2OH]_2\cdot 5H_2O$ (**2**)

(a) Compound **1**

Bond Distances

Cr–O1	1.957 (2)	Cr–N1	2.047 (2)
Cr–O2	1.949 (2)	Cr–N2	2.053 (2)
Cr–O3	1.950 (2)	Cr–N3	2.058 (2)

Bond Angles

O1–Cr–O2	175.51 (7)	O2–Cr–N3	88.73 (8)
O1–Cr–O3	94.31 (7)	O3–Cr–N1	90.45 (7)
O1–Cr–N1	80.32 (8)	O3–Cr–N2	170.83 (8)
O1–Cr–N2	94.79 (7)	O3–Cr–N3	81.21 (7)
O1–Cr–N3	92.34 (7)	N1–Cr–N2	92.24 (7)
O2–Cr–O3	90.16 (7)	N1–Cr–N3	168.49 (8)
O2–Cr–N1	99.28 (8)	N2–Cr–N3	97.24 (8)
O2–Cr–N2	80.75 (7)		

(b) Compound **2**

Bond Distances

Cr1–Cr2	2.999 (1)	Cr2–O1	1.963 (3)
Cr1–O1	1.980 (3)	Cr2–O2	1.934 (3)
Cr1–O2	1.937 (3)	Cr2–O7	1.958 (3)
Cr1–O3	1.975 (3)	Cr2–O9	1.964 (3)
Cr1–O5	1.958 (3)	Cr2–N3	2.048 (4)
Cr1–N1	2.065 (3)	Cr2–N4	2.066 (4)
Cr1–N2	2.068 (3)	O1–O2	2.503 (4)

Bond Angles

O1–Cr1–O2	79.43 (12)	O1–Cr2–O7	93.26 (12)
O1–Cr1–O3	92.00 (12)	O1–Cr2–O9	93.22 (11)
O1–Cr1–O5	172.21 (12)	O1–Cr2–N3	169.58 (12)
O1–Cr1–N1	93.22 (12)	O1–Cr2–N4	95.08 (13)
O1–Cr1–N2	99.07 (12)	O2–Cr2–O7	95.69 (12)
O2–Cr1–O3	171.20 (12)	O2–Cr2–O9	93.02 (12)
O2–Cr1–O5	92.81 (12)	O2–Cr2–N3	92.57 (14)
O2–Cr1–N1	97.99 (12)	O2–Cr2–N4	171.32 (12)
O2–Cr1–N2	93.35 (12)	O7–Cr2–O9	169.94 (14)
O3–Cr1–O5	95.77 (12)	O7–Cr2–N3	80.21 (13)
O3–Cr1–N1	80.34 (12)	O7–Cr2–N4	91.65 (13)
O3–Cr1–N2	89.97 (12)	O9–Cr2–N3	94.39 (13)
O5–Cr1–N1	88.61 (12)	O9–Cr2–N4	80.11 (12)
O5–Cr1–N2	80.46 (12)	N3–Cr2–N4	93.24 (15)
N1–Cr1–N2	164.62 (15)	Cr1–O1–Cr2	99.05 (12)
O1–Cr2–O2	79.92 (12)	Cr1–O2–Cr2	101.59 (12)

Table IV. Comparison of Metal–Ligand Bond Lengths for $M(pic)_3\cdot H_2O$

bond, Å	$Cr(pic)_3$[a]	$Mn(pic)_3$[23]	$Co(pic)_3$[12]
M–O1	1.957 (2)	1.891 (5)	1.88 (2)
M–O2	1.949 (2)	1.908 (5)	1.89 (2)
M–O3	1.950 (2)	1.942 (5)	1.89 (1)
M–N1	2.047 (2)	2.059 (5)	1.92 (1)
M–N2	2.053 (2)	2.217 (5)	1.92 (1)
M–N3	2.058 (2)	2.254 (6)	1.93 (2)
atomic radii,[24] Å	Cr(III)	Mn(III) hs	Co(III) ls
	0.755	0.785	0.685

[a] This work.

(21) Nakahara, M. *Bull. Chem. Soc. Jpn.* **1962**, *35*, 782–785.
(22) Cotton, F. A.; Wilkinson, G.; *Advanced Inorganic Chemistry*, 5th ed.; John Wiley and Sons: New York, 1988; p 689.
(23) Figgis, B. N.; Raston, C. L.; Sharma, R. P.; White, A. H. *Aust. J. Chem.* **1978**, *31*, 2545–2548.
(24) Shannon, R. D. *Acta Crystallogr., Sect. A* **1976**, 751–767.
(25) Folting, K.; Cox, M. M.; Moore, J. W.; Merritt, L. L. *J. Chem. Soc., Chem. Commun.* **1968**, 1170–1171.

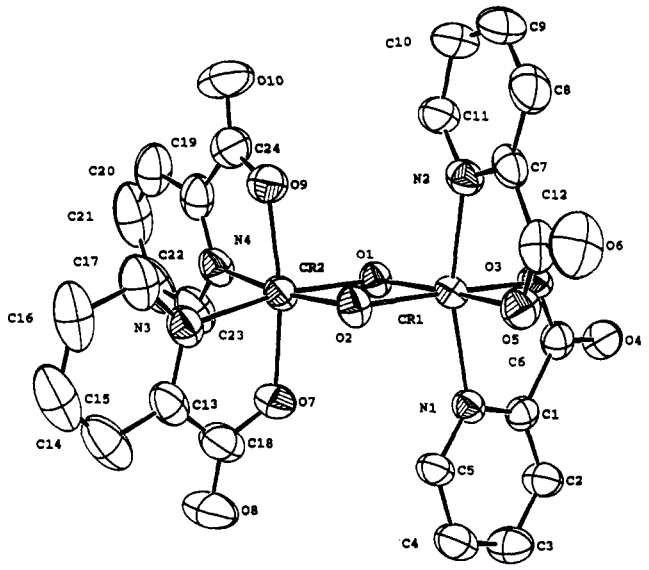

Figure 3. Molecular structure of $[Cr(pic)_2OH]_2$ (**2**). Thermal ellipsoids are at 50% probability. Hydrogen atoms and oxygen atoms of solvating water are omitted for clarity.

is 2.999 (1) Å, and the Cr–O bridge distances range from 1.934 (3) to 1.980 (3) Å. The Cr–O–Cr bridging angles are 99.0 (1) and 101.6 (1)°, and the O–Cr–O angles are 79.4 (1) and 79.9 (1)°. These parameters are within the ranges of the core distances and angles for the 26 previously characterized bis(μ-hydroxo)-bridged dimers,[14,26-48] which are as follows: Cr–Cr, 2.949–3.086 Å; Cr–OH, 1.911–1.988 Å; Cr–O–Cr, 97.57–104.08°; O–Cr–O, 75.92–82.40°. The Cr–O carboxylate ligand distances for **2** range from 1.958 (3) to 1.975 (3) Å, and the Cr–N distances range from 2.048 (4) to 2.068 (3) Å.

There is no crystallographically imposed symmetry in the dimer; however, there is pseudo-2-fold rotation symmetry along the Cr–

(26) Andersen, P.; Dossing, A.; Larson, S. *Acta Chem. Scand.* **1990**, *44*, 455–458.
(27) Gafford, B. G.; Holwerda, R. A. *Inorg. Chem.* **1989**, *28*, 60–66.
(28) Hodgson, D. J.; Zietlow, M. H.; Pedersen, E.; Toftlund, H. *Inorg. Chim. Acta* **1988**, *149*, 111–117.
(29) Teixidor, F.; Colomer, J.; Casabo, E.; Molins, C.; Miravitlles, C.; Palacio, F. *Inorg. Chim. Acta* **1988**, *147*, 151–157.
(30) Spiccia, L.; Stoeckli-Evans, H.; Marty, W.; Giovanoli, R. *Inorg. Chem.* **1987**, *26*, 474–482.
(31) Hodgson, D. J.; Pedersen, E.; Toftlund, H.; Weiss, C. *Inorg. Chim. Acta* **1986**, *120*, 177–184.
(32) Fischer, H. R.; Hodgson, D. J.; Michelsen, K.; Pedersen, E. *Inorg. Chim. Acta* **1984**, *88*, 143–150.
(33) Heinrichs, M. A.; Hodgson, D. J.; Michelsen, K.; Pedersen, E. *Inorg. Chem.* **1984**, *23*, 3174–3180.
(34) Cline, S. J.; Hodgson, D. J.; Kallesøe, S.; Larsen, S. *Inorg. Chem.* **1983**, *22*, 637–642.
(35) Larsen, S.; Hansen, B. *Acta Chem. Scand.* **1981**, *A35*, 105–110.
(36) Ranger, G.; Beauchamp, A. L. *Acta Crystallogr., Sect. B* **1981**, *B37*, 1063–1067.
(37) Lethbridge, J. W. *J. Chem. Soc., Dalton Trans.* **1980**, 2039–2041.
(38) Srdanov, G.; Herak, R.; Radanovic, D. J.; Veselinovic, D. S. *Inorg. Chim. Acta* **1980**, *38*, 37–42.
(39) Beutler, A.; Güdel, H. U.; Snellgrove, T. R.; Chapuis, G.; Schenk, K. J. *J. Chem. Soc., Dalton Trans.* **1979**, 983–992.
(40) Cline, S. J.; Kallesøe, S.; Pedersen, E.; Hodgson, D. J. *Inorg. Chem.* **1979**, *18*, 796–801.
(41) Cline, S. J.; Scaringe, R. P.; Hatfield, W. E.; Hodgson, D. J. *J. Chem. Soc., Dalton Trans.* **1977**, 1662–1666.
(42) Ou, C. C.; Borowski, W. J.; Potenza, J. A.; Schugar, H. J. *Acta Crystallogr., Sect. B* **1977**, *B33*, 3246–3248.
(43) Scaringe, R. P.; Hatfield, W. E.; Hodgson, D. J. *Inorg. Chem.* **1977**, *16*, 1600–1605.
(44) Scaringe, R. P.; Hatfield, W. E.; Hodgson, D. J. *Inorg. Chim. Acta* **1977**, *22*, 175–183.
(45) Kaas, K. *Acta Crystallogr., Sect. B* **1976**, *B32*, 2021–2025.
(46) Scaringe, R. P.; Singh, P.; Eckberg, R. P.; Hatfield, W. E.; Hodgson, D. J. *Inorg. Chem.* **1975**, *14*, 1127–1133.
(47) Veal, J. T.; Hatfield, W. E.; Hodgson, D. J. *Acta Crystallogr., Sect. B* **1973**, *B29*, 12–20.
(48) Veal, J. T.; Hatfield, W. E.; Jeter, D. Y.; Hempel, J. C.; Hodgson, D. J. *Inorg. Chem.* **1973**, *12*, 342–346.

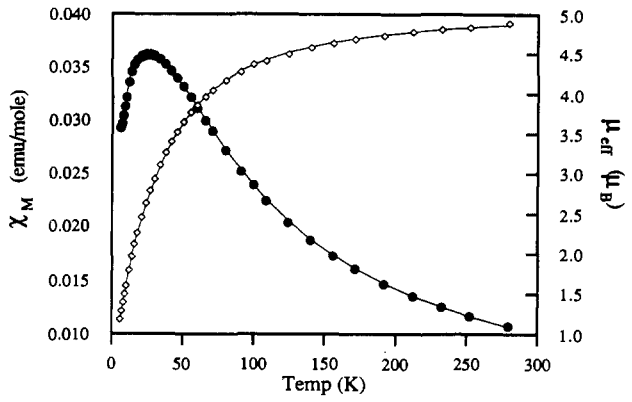

Figure 4. Variable-temperature-measured magnetic susceptibility of $[Cr(pic)_2OH]_2$ (**2**): (●) χm; (—) χm(calc); (◇) μ_{eff}, (—) $\mu_{eff(calc)}$ as a function of temperature.

Cr axis. It is of interest to note the axial vs equatorial coordination of the picolinate ligands for each chromium atom. On one side of the dimer (Cr1) the pyridine rings are trans to one another and cis to the bridging hydroxide groups; on the other side (Cr2) they are cis to one another and trans to the bridging hydroxide groups. There is no apparent difference in the Cr–N and Cr–O bond lengths (trans effect) for cis vs trans coordination relative to the bridging plane. This is not surprising since the Cr–OH bond distances are relatively long. This same coordination is observed with bis(μ-hydroxo)tetrakis(L-prolinato)dichromium(III).[14] However, a different coordination is observed with bis(μ-hydroxo)-tetrakis[1-(2-pyridyl)ethylamine]dichromium(III)[35] even though the 1-(2-pyridyl)ethylamine ligand has the same chelation geometry as picolinate. In that case each of the two sets of pyridine rings are coordinated trans to each other and cis to the bridging hydroxide groups. The geometry of the prolinato dimer was rationalized in terms of the intramolecular hydrogen bonding. This argument cannot be made for the picolinate dimer.

There is no disorder in the chromium complex itself. The disordered lattice water molecules are in the region of O6 (by 2.7–2.8 Å) and O8 (by 2.5–2.9 Å). There is no apparent hydrogen bonding to the bridging hydroxide groups.

Magnetic Properties. The solid-state room temperature magnetic moment for **1**, 3.88 (3) μ_B, is in agreement with the moment of 3.84 μ_B measured by Dorsett and Walton,[10] as expected for a magnetically dilute $S = {}^3/_2$ system.

Variable-temperature solid state magnetic susceptibility measurements for **2** were made on a powdered anhydrous sample in the temperature range 6–280 K. The data were fitted to the following expression for χ_m vs T derived from the isotropic spin-exchange Hamiltonian $\mathcal{H} = -2J\hat{S}_1\cdot\hat{S}_2$ with $S_1 = S_2 = {}^3/_2$[19]

$$\chi = \frac{Ng^2\mu_B{}^2[2e^{2x} + 10e^{6x} + 28e^{12x}]}{kT[1 + 3e^{2x} + 5e^{6x} + 7e^{12x}]} + \frac{C_{pi}}{T}$$

where $x = J/kT$, and C_{pi} = paramagnetic impurity factor.

The effective magnetic moment for **2** decreases from 4.89 μ_B at 280 K to 1.18 μ_B at 6 K (Figure 4). At 280 K this corresponds to a μ_{eff}/Cr of 3.46 μ_B, which is lower than that expected for a magnetically isolated d^3 ion (3.87 μ_B). A poor fit to the data was obtained with a fixed g value of 2.0023 giving $J = -10.4$ (5) cm^{-1} and a paramagnetic impurity of 3.02 mol % (assuming an impurity of monomeric Cr, $S = {}^3/_2$), with an agreement factor R of 0.010, where $R = [\Sigma(\chi_M^{exp} - \chi_M^{calc})^2]/\Sigma(\chi_M^{exp})^2$. The best fit (Figure 4) resulted from refinement of J, g, and paramagnetic impurity, giving $J = -8.02$ (4) cm^{-1}, $g = 1.844$, a paramagnetic impurity of 2.23 (4) mol %, and $R = 4.8 \times 10^{-5}$.

There was no improvement in the fit upon including a biquadratic exchange constant where $\mathcal{H} = -2J\hat{S}_1\cdot\hat{S}_2 + j(\hat{S}_1\cdot\hat{S}_2)^2$ and the energies of the triplet, quintet, and septet states are $(2J - 6.5j)$, $(6J - 13.5j)$, and $(12J - 9j)$, respectively. This gives J

$= -8.31$ (11) cm^{-1}, $j = -0.17$ (1) cm^{-1}, $g = 1.852$, a paramagnetic impurity of 2.05 (7) mol %, and $R = 8.1 \times 10^{-5}$. Refinement of J and g alone gives best fit parameters of $J = -5.74$ (11) cm^{-1}, $g = 1.816$ (2), and $R = 5.8 \times 10^{-3}$.

It is not possible to fit the structural parameters for **2** to the full GHP equation[17] because the positions of the bridging hydroxide protons were not refined; therefore, θ is not known with accuracy. However, using the averages for r and ϕ, and the experimentally determined J of -8.02 cm^{-1}, corresponding to a triplet energy of 16 cm^{-1} above the ground state, the GHP equation predicts a reasonable value for θ of 40°. The GHP model predicts weaker Cr–Cr coupling for larger values of θ which corresponds to the p orbital on the bridging oxygen atom being farther from perpendicular to the Cr–O–Cr plane, resulting in less magnetic interaction between metal atoms.

Biological Relevance. A biological role for chromium was first proposed by Mertz[2a] who found the impairment of glucose tolerance in rats fed a chromium deficient diet. Glucose tolerance was restored by adding chromium supplements. A biological chromium complex, termed the glucose tolerance factor (GTF), was postulated to function as a cofactor for insulin potentiation. The most active form of GTF is isolated from brewer's yeast.[49] Mertz has proposed[50a,b] that it contains chromium, two molecules of nicotinic acid, glycine, glutamic acid, and cysteine. The nicotinic acid ligands have been assigned as binding through the pyridine nitrogens in a trans configuration.[50a] This assignment appears to be based on comparison to the one nicotinate–transition metal complex known at that time, that of cobalt(II),[51] which is not necessarily relevant to the chromium(III) case. Coordination of nicotinate to chromium through the carboxylate oxygen atoms has been shown for the oxo-bridged trinuclear species[6b] and a mononuclear complex.[52a,b] It has been suggested that the oxo-bridged trinuclear core may be present in GTF in vivo.[6b]

The exact identity, and indeed even the existence of a chromium-containing GTF, has yet to be determined unequivocally and there is much controversy surrounding its characterization and biological function. Some studies have found that the biologically active component does not contain chromium;[53a,b] others have found that nicotinic acid is not necessary.[54a,b] Some authors have presented evidence that isolated GTF binds insulin,[55] while others have reported that it will not bind.[56] A proposal has been made that it functions not as an insulin cofactor, but in transport of sugar into cells.[57a,b] Another study suggests that GTF stimulates glycolysis, however not through increased transport of sugar into cells.[58]

Regardless of the lack of understanding of the function and structure of the proposed glucose tolerance factor, there is the related area of study that shows many cases of improved glucose tolerance and blood lipid metabolism in humans and animals following the administration of chromium complexes.[50a,59a,b] But there are many different forms of chromium-containing dietary supplements currently available to consumers, with varying degrees of demonstrated biological activity. Therefore, there is much interest in understanding how the coordination environment affects chromium's biological activity.

Several studies report the observation of a lag time between the administration of isolated GTF or inorganic chromium supplements and the improvement of glucose tolerance,[54b,57,58] suggesting that conversion to a more active form takes place. The complex of chromium with a given ligand may not be a model for the actual glucose tolerance factor per se, yet that ligand may play a role in biological uptake, utilization, and/or conversion to the GTF form.

A number of studies have been conducted to determine the relative biological activity and absorption of inorganic chromium complexes,[60] one of the most notable being that of Gonzalez and co-workers[60a] which showed differences up to a factor of 40 for the liver retention of a number of chromium Schiff base complexes. From the differing rates of excretion they concluded that the chromium remained chelated. However, since neither this study nor the other studies[60b-d] included structurally characterized molecules,[61] there are limits to the conclusions that can be drawn about the mechanism of chromium absorption.

The relevance of picolinate complexes to biologically active chromium and its safe use as a dietary supplement have not been established. Although Evans and co-workers report a role for $[Cr(pic)_3]$ in the maintenance of normal lipid and carbohydrate metabolism,[3b] Mertz and others found chromium picolinate did not potentiate insulin in rat epididymal fat tissue,[50a] and picolinic acid has been shown to alter iron metabolism.[62] We are interested in picolinic acid as one of many ligands that can be used to study the effect of structure on chromium metabolism and the extent, if any, to which this activity can be controlled by choice of ligand.

Concluding Remarks

Two products from the aqueous reaction mixtures of chromium(III) with picolinic acid have been structurally characterized. The red monomeric species has been found to be the meridional isomer of $[Cr(pic)_3]$, not the facial isomer as conjectured previously.[7,9] The second product is the purple binuclear species $[Cr(pic)_2OH]_2$. Prior to this work the structure of $[Cr(pic)_3]$ had been assigned solely by comparison of the compound's color with that of previously determined complexes.[11-13] Since the tris(picolinate) complexes of chromium(III), cobalt(III),[12] and manganese(III)[23] are isostructural, this serves as an example of the importance of the ligand's effect on conformational stability over any assumed preference of the metal.[14]

Chromium tris(picolinate) has been proposed to provide a biologically active source of chromium in humans.[3a,b] Now that its structure and that of the hydrolysis product have been established, work is in progress to examine its bioavailability as

(49) Toepfer, E. W.; Roginski, E. E.; Polansky, M. M. *J. Agr. Food Chem.* **1973**, *21*, 69–73.
(50) (a) Mertz, W.; Toepfer, E. W.; Roginski, E. E.; Polansky, M. M. *Fed. Proc.* **1974**, *33*, 2275–2289. (b) Toepfer, E. W.; Mertz, W.; Polansky, M. M.; Roginski, E. E.; Wolf, W. R. *J. Agr. Food Chem.* **1977**, *25*, 162–166.
(51) Anagnostopoulos, A. M.; Drew, G. B.; Walton, R. A. *J. Chem. Soc.* **1969**, 1241–1242.
(52) (a) Bouma, R. J.; Teuben, J. H.; Beukema, W. R.; Bansemer, R. L.; Huffman, J. C.; Caulton, K. G. *Inorg. Chem.* **1984**, *23*, 2715–2718. (b) Chang, J. C.; Gerdom, L. E.; Baenziger, N. C.; Goff, H. M. *Inorg. Chem.* **1983**, *22*, 1739–1744.
(53) (a) Haylock, S. J.; Buckley, P. D.; Blackwell, L. F. *J. Inorg. Biochem.* **1983**, *19*, 105–117. (b) Hwang, D. L.; Lev-Ran, A.; Papoian, T., Beech, W. K. *J. Inorg. Biochem.* **1987**, *30*, 219–225.
(54) (a) Cooper, J. A.; Blackwell, L. F.; Buckley, P. D. *Inorg. Chim. Acta* **1984**, *92*, 23–31. (b) Yamamoto, A.; Wada, O.; Ono, T. *Eur. J. Biochem.* **1987**, *165*, 627–631.
(55) Evans, G. W.; Roginski, E. E.; Mertz, W. *Biochem. Biophys. Res. Commun.* **1973**, *50*, 718–722.
(56) Kumpulainen, J.; Koivistoinen, P.; Lahtinen, S. *Bioinorg. Chem.* **1978**, *8*, 419–429.
(57) (a) Mirsky, N.; Weiss, A.; Dori, Z. *J. Inorg. Biochem.* **1981**, *15*, 275–279. (b) Mirsky, N.; Weiss, A.; Dori, Z. *J. Inorg. Biochem.* **1980**, *13*, 11–21.
(58) Holdsworth, E. S.; Appleby, G. *J. Inorg. Biochem.* **1984**, *21*, 31–44.
(59) (a) Anderson, R. A. In *Modern Nutrition in Health and Disease*, 7th ed.; Shils, M. E., Young, V. R., Eds.; Lea and Febiger: Philadelphia, PA 1988; pp 268–273. (b) Borel, J. S.; Anderson, R. A. In *Biochemistry of the Elements*; Frieden, E., Ed.; Plenum Press: New York, 1984; pp 175–199.
(60) (a) Gonzalez-Vergara, E.; De Gonzalez, B. C.; Hegenauer, J.; Saltman, P. *Isr. J. Chem.* **1981**, *21*, 18–22. (b) Votava, H. J.; Hahn, C. J.; Evans, G. W. *Biochem. Biophys. Res. Commun.* **1973**, *55*, 312–319. (c) Mertz, W. *Nutr. Rev.* **1975**, *33*, 129–135. (d) Mertz, W.; Roginski, E. E.; Schwarz, K. *J. Biol. Chem.* **1961**, *236*, 318–322.
(61) A biological reactivity study has been carried out with the structurally characterized complex $[Cr^{II}(nic)_2(H_2O)_4]$: Cooper, J. A.; Anderson, B. F.; Buckley, P. D.; Blackwell, L. F. *Inorg. Chim. Acta* **1984**, *91*, 1–9. However, the later discovery of contamination with $[Zn(nic)_2(H_2O)_4]$ renders their results questionable. See: Broderick, W. E.; Pressprich, M. R.; Geiser, U.; Willett, R. D.; Legg, J. I. *Inorg. Chem.* **1986**, *25*, 3372–3377.
(62) Fernandez-Pol, J. *Biochem. Biophys. Res. Commun.* **1977**, *78*, 136–143.

well as that of other chromium complexes in an attempt to further define what effect ligand environment may have on the uptake and biological activity of chromium.

Acknowledgment. Support for this work was provided by a University of California, Berkeley, Biomedical Research Support Grant. We thank Joel Gohdes and Steve Keller for magnetic susceptibility measurements, Dr. Frederick J. Hollander for assistance with the crystal structure determinations, and William Seroy for helpful discussions.

Supplementary Material Available: Tables giving a full listing of crystallographic data, anisotropic thermal parameters, bond distances and angles, and hydrogen atom parameters for **1** and **2**, least squares planes for **1**, and magnetic data for **2** and crystal packing diagrams for **1** and **2** (12 pages). Ordering information is given on any current masthead page.